

## Analysis of Electron Temperature in DC Ar/SF<sub>6</sub> Plasma Using Cylindrical and Planar Probes

Jin-Woo Kim<sup>1,2</sup>, Soon-Gook Cho<sup>1,2</sup>, Min-Keun Bae<sup>1,2</sup>, Hyung-Jin Kim<sup>1,2</sup>, Tae Hun Chung<sup>3</sup>, and Kyu-Sun Chung<sup>1,2\*</sup>

<sup>1</sup>Center for Edge Plasma Science, Hanyang University, Seoul 133-791, Korea

<sup>2</sup>Department of Electrical Engineering, Hanyang University, Seoul 133-791, Korea

<sup>3</sup>Department of Physics, Dong-A University, Busan 604-020, Korea

Received April 4, 2013; accepted July 25, 2013; published online November 20, 2013

Electronegative plasmas are generated by adding SF<sub>6</sub> gas to a background argon (Ar) DC plasma with parameters of  $n_0 = 1 \times 10^{10} \text{ cm}^{-3}$  and  $T_e = 2 \text{ eV}$ . The heating current of the thoriated filament was in the range of 20.5–21.5 A and the plasmas were generated under a discharge condition of 100 V/0.4 A. The amount of negative ions was controlled by adjusting the ratio of flow rate of SF<sub>6</sub> = 0–10% to that of Ar. Plasma parameters were measured using cylindrical and planar electric probes. The behavior of electrons, which means the change in a parameter due to negative ion production, is characterized by measuring the floating and plasma potentials, and electron temperature. Electron temperature seems to increase and the potentials decrease with SF<sub>6</sub> flow rate. © 2013 The Japan Society of Applied Physics

### 1. Introduction

Negative ions have been widely observed in various plasmas such as processing,<sup>1–3</sup> nuclear fusion,<sup>4–8</sup> accelerators,<sup>8,9</sup> materials science applications.<sup>10</sup> Owing to the weak bonding of electrons to heavy neutral atoms or molecules among single positive-charged ions and electrons, it is not easy to characterize the negative ions, although there have been various methods to measure them such as optical emission spectroscopy (OES),<sup>11</sup> the laser photodetachment (LPD) method,<sup>2,12,13</sup> the ion acoustic wave (time-of-flight) method (IAW)<sup>15–17</sup> and the use of electric probes.<sup>11,14,17–26</sup> For conventional methods using electric probes and OES, fully ionized plasma with singly positive-charged ions and a Boltzmann electron with one thermal temperature are assumed. In the LPD method, there is a need to define the cross section of a high-power laser beam, which often ionizes the neutral gas leading to the generation of electrons, which which contaminate the detached electrons purely generated from negative ions. The IAW method requires the effective mass of the ions, which contains an unknown ratio of density of the negative ions to that of the background positive ions.

In this work, negative ions were generated by adding SF<sub>6</sub> gas to a background argon (Ar) DC plasma with a thoriated filament. The amount of negative ions was controlled by adjusting the ratio of the flow rate of SF<sub>6</sub> gas to that of Ar gas. Plasma parameters were measured using cylindrical and planar probes. Since the changes in plasma parameters related to electron and electron energy distributions before and after negative ion production are also meaningful from the viewpoint of quasi-neutrality, electron behavior is characterized on the basis of the floating potential, plasma potential, electron temperature, and electron energy distribution function (EEDF) by analyzing current–voltage characteristics.

### 2. Experimental Procedure

Experiments were performed in a thoriated tungsten filament DC plasma. Figure 1 shows a schematic view of the plasma chamber 50 cm in diameter and 80 cm in length, which has permanent magnets in the azimuthal direction. Four lines

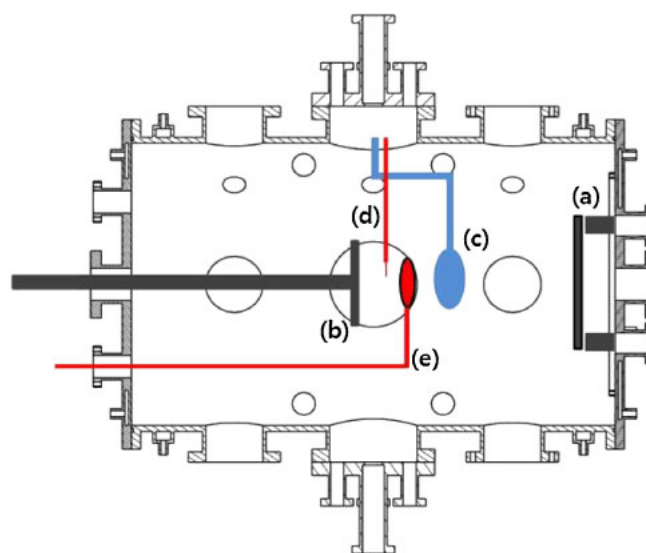


**Fig. 1.** (Color online) Schematic view of DC filament plasma experiment: (a) cathode (thoriated tungsten), (b) a target, (c) a stainless-steel grid, (d) a cylindrical single probe, and (e) a single planar probe. The chamber wall is biased positively with respect to the cathode.

of filament with a diameter of 0.25 mm were installed in parallel. A target was installed in the floating state in order to concentrate the plasma between the source and target. A floating stainless-steel grid was installed for another ion acoustic wave experiment; the grid seems to partially block the primary energetic electrons. Two electric probes were installed: one is a single cylindrical probe made of molybdenum with a tip 0.5 mm in diameter and 3 mm in length, and the other is a single planar probe made of circular tungsten plate 6 mm in diameter.

The base pressure was about  $6.6 \times 10^{-7}$  Torr and the operating pressure was  $(2.4–2.6) \times 10^{-4}$  Torr. The filaments were heated up by a current of 20.5–21.5 A and the plasma was generated under a discharge condition of 100 V/0.4 A. The amount of negative ions was controlled by adjusting the ratio of gas flow rates to be within the ranges of Ar = 90–100% and SF<sub>6</sub> = 0–10% by letting the total gas flow be

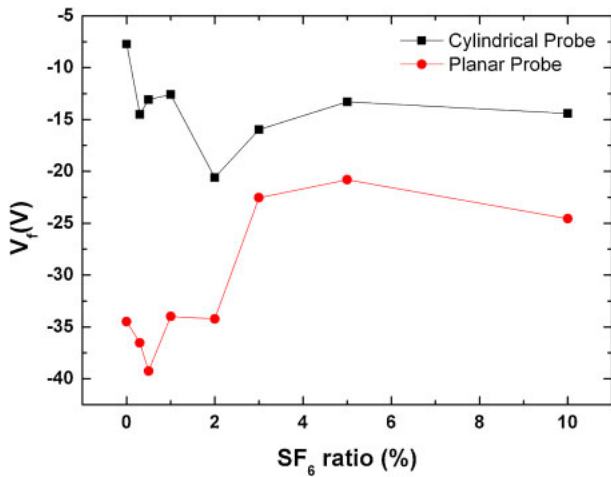


Fig. 2. (Color online) Floating potential ( $V_f$ ).

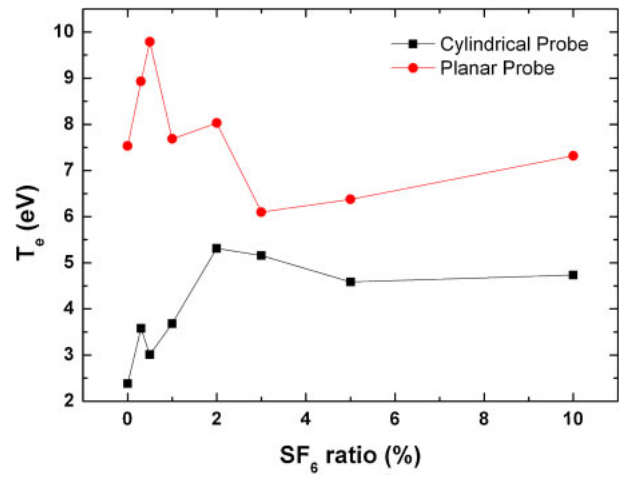


Fig. 4. (Color online) Electron temperature ( $T_e$ ).

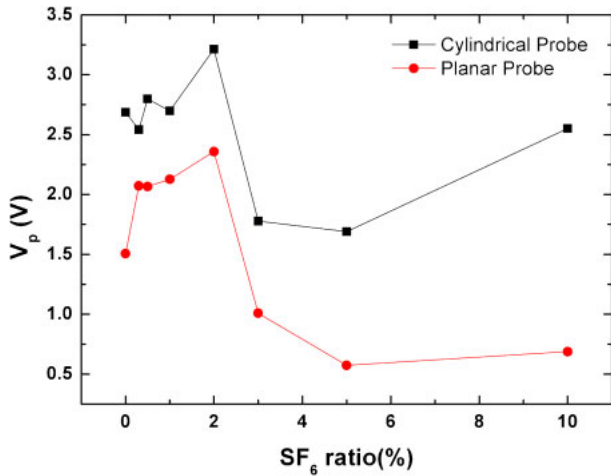


Fig. 3. (Color online) Plasma potential ( $V_p$ ).

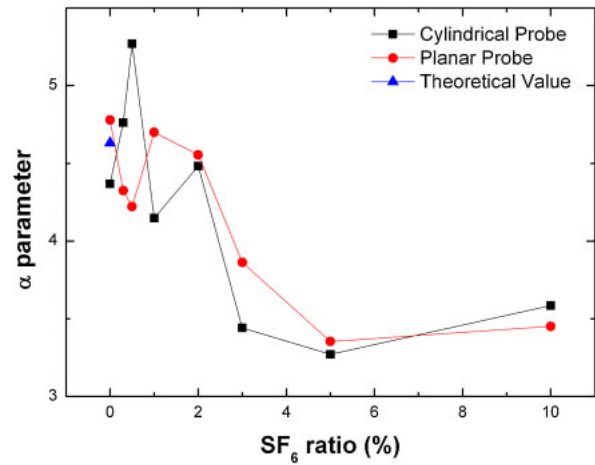


Fig. 5. (Color online)  $\alpha$  parameter.

fixed to 1.23 sccm. Typical parameters of the background Ar plasma were  $n_0 \sim 10^{10} \text{ cm}^{-3}$  and  $T_e \sim 2 \text{ eV}$ .

### 3. Results and Discussion

Thermionic electrons are emitted by thermionic emission from thoriated tungsten filaments according to the Richardson(-Dushman) formula.<sup>27)</sup> These thermionic electrons are accelerated by the potential difference between the cathode and the chamber wall (anode) biased at 100 V. So that the energetic primary electrons hit the argon neutrals to be ionized. During ionization, a large number of electrons are also thermalized by Coulomb collision and become thermal electrons. Figures 2 and 3 show the floating and plasma potentials measured using two electric probes. The plasma potentials of both probes show similar trends: they tended to decrease at low SF<sub>6</sub> ratios (0–3%) and saturate at relatively high SF<sub>6</sub> ratios (3–10%). The floating potentials of the cylindrical probe seem to decrease with SF<sub>6</sub> ratio, while those of the planar probe increase, which are not easy to understand. One would expect that floating potential decreases with SF<sub>6</sub> gas flow rate, i.e., with the increase in the density of negative ions. Low-energy electrons are used to generate negative ions, so that the velocity (and energy)

distribution would broaden, leading to the increase in electron temperature. However, both the plasma and floating potentials of the planar probe are lower than those of the cylindrical probe, which indicates that energetic primary electrons shift the whole current–voltage ( $I$ – $V$ ) curves to the negative direction, because the cylindrical probe is located within the wake of the planar probe in terms of the filament plasma source. The floating grid located between the filament source and the planar probe does not seem to block all of the energetic primary electrons, although a proportion of the energetic thermal electrons might be prevented from passing through it. If one assumes that the electrons have one thermal temperature due to one Maxwellian electron distribution, the relationship between the plasma and floating potentials can be described as<sup>28)</sup>

$$\alpha \equiv \frac{e|V_f - V_p|}{T_e} = 0.5 \ln \left[ \left( 2\pi \frac{m_e}{m_i} \right) \left( 1 + \frac{T_i}{T_e} \right) (1 - \gamma_e)^{-2} \right]^{-1}. \quad (1)$$

Figures 4 and 5 show the electron temperature and  $\alpha$  parameter, respectively. Since our plasma has a low density and a low electron temperature, we assumed  $\gamma_e$  (secondary

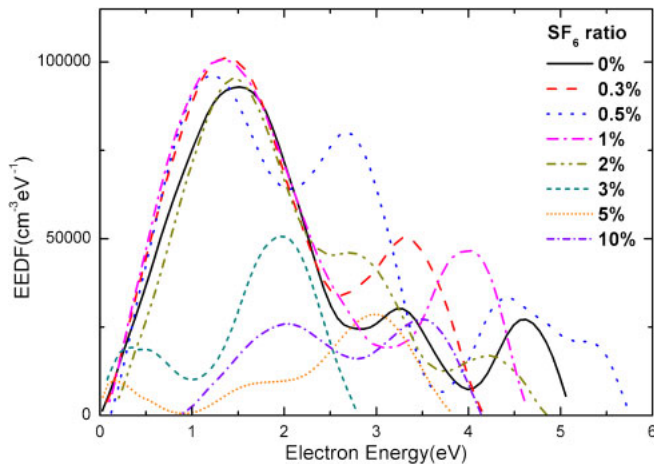


**Fig. 6.** (Color online) Electron energy density function measured using cylindrical probe.

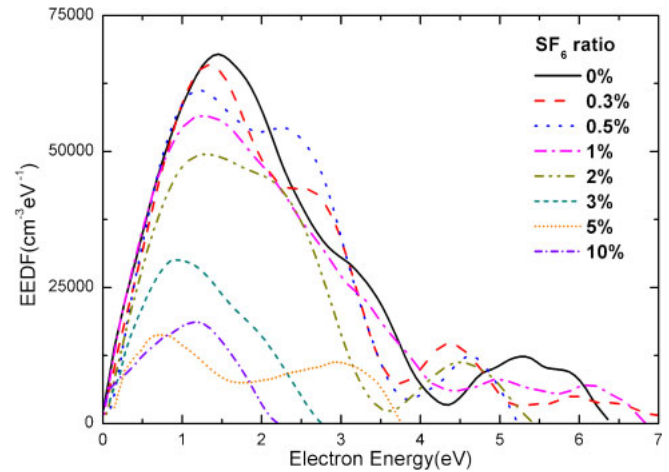


**Fig. 7.** (Color online) Electron energy density function measured using planar probe.

electron coefficient) = 0 and  $T_i/T_e = 0.1$ . Electron temperatures were deduced from the  $I$ - $V$  characteristics, assuming that a Boltzmann electron have one thermal temperature. It is suspected that the planar probe was still affected by energetic primary electrons owing to the high bias voltage ( $\sim 100$  V), although the floating grid partially blocked the energetic electrons. The electron temperature of each probe seems to have the opposite trend of  $V_f$ . It means that the behavior of hot primary electrons was dominant for the determination of electron temperature. The number of primary electrons tended to decrease with the number of negative ions. From the given  $T_e$  range, we would expect that negative ions could be generated by electron attachment.<sup>9,29,30</sup> It could be assumed that electrons with an energy lower than 1 eV are consumed by their attachment to  $SF_6$ . We could finally calculate the  $\alpha$  parameter and also confirm that the probes measured the same plasma we generated even when the other parameters seem to be markedly different. The tendency of the  $\alpha$  parameter to decrease can mean both the decrease in potential energy and the increase in electron thermal energy, since the  $\alpha$  parameter is the ratio of potential energy to electron thermal energy, as shown by Eq. (1). Figures 6 and 7 show the electron energy density functions (EEDFs). At least three groups of electrons were observed at approximately 1.5, 3, and 5.3 eV. The same trend is observed, that is, the density of electrons at approximately 3 eV increases and the density of electrons at approximately 1 eV decreases. Therefore, the changes in  $T_e$  may also be explained as follows;  $T_e$  measured using both probes can be explained by the decrease in the density of electrons having an energy lower than 1 eV and higher than 5.3 eV, and the increase in the density of another electron group at approximately 3 eV. We can also confirm that the  $\alpha$  parameter changes with the increase in electron thermal energy.

The plasma potential of each probe, as shown in Fig. 3, has the same tendency, that is, it increases until the  $SF_6$  ratio reaches 2% and then decreases. The increase can also be explained by the shift of electron energy. The decrease can be explained if the absolute electron density decreases. The plasma potential tended to saturate after reaching a  $SF_6$

ratio of 3% and the EEDFs after reaching the ratio of 3% are a little ambiguous.

$V_f$  measured using the planar probe is much lower than that measured using the cylindrical probe. It could be due to the energetic primary electrons (with a bias voltage of 100 V) from the filament plasma source. The behavior of the main thermal electrons can be determined using the cylindrical probe, that is,  $V_f$  tends to decrease at low  $SF_6$  ratios (0–3%) and to saturate at relatively high  $SF_6$  ratios (3–10%)-energetic primary electrons seem to be blocked by the planar probe.

#### 4. Conclusion

Experiments using mixed gases (Ar and  $SF_6$ ) were performed to characterize the electronegative plasmas. In particular, electron behavior was analyzed to determine the effect of electrons during negative ion production. The effects of the thermal and primary electrons induced by the probe array were analyzed on the basis of floating and plasma potentials, electron temperature, and EEDF. From the data of the ratios of potential energy to electron thermal energy ( $\alpha$ ), we confirmed the consistency of the measurement of electric probes, although the initial arrangement of the probe position seemed to be improved. The decrease in  $\alpha$  suggests either the increase in one thermal electron temperature or the generation of nonthermal electrons with different energy components, as shown by the data of EEDFs. The electron energy shift and decrease in density are observed from the EEDFs of the two probes. The decrease in the amount of low-energy electrons that generate negative ions seems to lead to the possible increase in electron energy and the decrease in the electron density.

#### Acknowledgements

This work was supported by the National R&D Program through the National Research Foundation of Korea (NRF) funded by the Ministry of Education, Science and Technology (2009-0082669). This work was partially supported by the R&D Program through the National Fusion Research Institute of Korea (NFRI) and the Korea Research Council of Fundamental Science and Technology.

- 1) T. Shibayama, H. Shindo, and Y. Horiike: *Plasma Sources Sci. Technol.* **5** (1996) 254.
- 2) A. Kono: *Appl. Surf. Sci.* **192** (2002) 115.
- 3) J. Ishikawa: *J. Korean Phys. Soc.* **48** (2006) 703.
- 4) L. R. Grisham: *Laser Part. Beams* **21** (2003) 545.
- 5) U. Fantz, P. Franzen, and D. Wunderlich: *Chem. Phys.* **398** (2012) 7.
- 6) Y. Okumura, Y. Fujiwara, T. Inoue, K. Miyamoto, N. Miyamoto, A. Nagase, Y. Ohara, and K. Watanabe: *Rev. Sci. Instrum.* **67** (1996) 1092.
- 7) S. I. Krashennnikov, A. Yu. Pigarov, and D. J. Sigmar: *Phys. Lett. A* **214** (1996) 285.
- 8) T. Inoue, M. Taniguchi, T. Morishita, M. Dairaku, M. Hanada, T. Imai, M. Kashiwagi, K. Sakamoto, T. Seki, and K. Watanabe: *Nucl. Fusion* **45** (2005) 790.
- 9) G. D. Alton: in *Electrostatic Accelerators*, ed. R. Hellborg (Springer, Heidelberg, 2005) Chap. 12.
- 10) J. Ishikawa: *Rev. Sci. Instrum.* **63** (1992) 2368.
- 11) A. M. Daltrini, S. A. Moshkalev, L. Swart, and P. B. Verdonck: *J. Integrat. Circuits Syst.* **2** (2007) 67.
- 12) L. St-Onge, M. Chaker, and J. Margot: *J. Vac. Sci. Technol. A* **18** (2000) 2363.
- 13) M. Bacal: *Rev. Sci. Instrum.* **71** (2000) 3981.
- 14) R. L. F. Boyd and J. B. Thompson: *Proc. R. Soc. London, Ser. A* **252** (1959) 102.
- 15) M. Shindo and Y. Kawai: *J. Phys. Soc. Jpn.* **70** (2001) 621.
- 16) A. Y. Wong, D. L. Mamas, and D. Arnush: *Phys. Fluids* **18** (1975) 1489.
- 17) M. Shindo, S. Uchino, R. Ichiki, S. Yoshimura, and Y. Kawai: *Rev. Sci. Instrum.* **72** (2001) 2288.
- 18) E. Stamate and K. Ohe: *J. Appl. Phys.* **84** (1998) 2450.
- 19) D. Boruah, A. R. Pal, H. Bailung, and J. Chutia: *J. Phys. D* **36** (2003) 645.
- 20) K.-S. Chung and S. Kado: *Phys. Plasmas* **13** (2006) 104509.
- 21) S. Y. Kang, T. H. Chung, and K.-S. Chung: *Rev. Sci. Instrum.* **80** (2009) 013502.
- 22) H. M. Joh, T. H. Chung, and K.-S. Chung: *Thin Solid Films* **518** (2010) 6686.
- 23) M. Tuszewski and R. R. White: *Plasma Sources Sci. Technol.* **11** (2002) 338.
- 24) E. Stamate and K. Ohe: *J. Appl. Phys.* **89** (2001) 2058.
- 25) T. K. Popov and S. V. Gateva: *Plasma Sources Sci. Technol.* **10** (2001) 614.
- 26) H. Amemiya: *J. Phys. D* **23** (1990) 999.
- 27) A. Y. Wong: *Introduction to Experimental Plasma Physics* (Physics Department, University of California at Los Angeles, 1977) Vol. 1, Chap. 1.
- 28) P. C. Stangeby: in *Physics of Plasma-Wall Interactions in Controlled Fusion*, ed. D. E. Post and R. Behrisch (Plenum, New York, 1986) p. 41.
- 29) L. G. Christophorou and J. K. Olthoff: *J. Phys. Chem. Ref. Data* **29** (2000) 267.
- 30) J. Ishikawa: in *The Physics and Technology of Ion Sources*, ed. I. G. Brown (Wiley-VCH, Weinheim, 2004) Chap. 14.